# Direct identification of NH⋯N hydrogen bonds in non-canonical base pairs of RNA by NMR spectroscopy

Jens Wöhnert, Andrew J. Dingley[1,2], Matthias Stoldt, Matthias Görlach*, Stephan Grzesiek[1,2] and Larry R. Brown

Abteilung Molekulare Biophysik/NMR-Spektroskopie, Institut für Molekulare Biotechnologie e. V. Jena, Postfach 100813, 07708 Jena, Germany, [1]Forschungszentrum Jülich, Institut für Strukturbiologie, IBI-2, 52425 Jülich, Germany and [2]Institut für Physikalische Biologie, Heinrich-Heine-Universität, 40225 Düsseldorf, Germany

## ABSTRACT

**It is shown that the recently developed quantitative $J_{NN}$ HNN-COSY experiment can be used for the direct identification of hydrogen bonds in non-canonical base pairs in RNA. Scalar $^{2h}J_{NN}$ couplings across NH⋯N hydrogen bonds are observed in imino hydrogen bonded GA base pairs of the hpGA RNA molecule, which contains a tandem GA mismatch, and in the reverse Hoogsteen AU base pairs of the E-loop of *Escherichia coli* 5S rRNA. These scalar couplings correlate the imino donor $^{15}N$ nucleus of guanine or uridine with the acceptor N1 or N7 nucleus of adenine. The values of the corresponding $^{2h}J_{NN}$ coupling constants are similar in size to those observed in Watson–Crick base pairs. The reverse Hoogsteen base pairs could be directly detected for the E-loop of *E.coli* 5S rRNA both in the free form and in a complex with the ribosomal protein L25. This supports the notion that the E-loop is a pre-folded RNA recognition site that is not subject to significant induced conformational changes. Since Watson–Crick GC and AU base pairs are also readily detected the HNN-COSY experiment provides a useful and sensitive tool for the rapid identification of RNA secondary structure elements.**

## INTRODUCTION

In addition to the formation of canonical A-form helices, RNA is able to adopt a wide range of non-canonical structures such as stable mismatched base pairs, bulges, base triples or tetrads and stable hairpin loops. Such structural elements contribute to the formation of higher order structures in RNA and are important sites for molecular recognition events related to the biological function of RNA molecules. In studies of RNA structure, it is of critical importance to identify the underlying hydrogen bonding patterns within non-canonical RNA motifs, i.e. the hydrogen bond donor and acceptor pairs. Usually, the existence of hydrogen bonds is inferred after the structure is solved by either X-ray crystallography or NMR, i.e. from spatial proximity and from the relative orientation of hydrogen bond donor and acceptor groups.

Recently, it was demonstrated that hydrogen bonds in Watson–Crick base pairs of RNA (1) and DNA (2) with imino groups as donors and nitrogens as acceptors can be detected directly by NMR spectroscopy, since the hydrogen bond gives rise to internucleotide trans-hydrogen bond $^{2h}J_{NN}$ and $^{1h}J_{HN}$ scalar couplings. More recently, scalar couplings ($^{3h}J_{NC'}$) across hydrogen bonds between the amide proton and the carbonyl $^{13}C$ nucleus could be observed in proteins (3). Although the chemical shifts and the exchange properties of imino/amino/amide hydrogens have often been used in NMR studies as indicators of hydrogen bonding, with subsequent incorporation as constraints in structural calculations, the direct detection of the donor and acceptor groups embodied by these new experiments is an important advance in NMR methodology.

For Watson–Crick base pairs in nucleic acids, the HNN-COSY experiment (1) utilizes the $^{2h}J_{NN}$ coupling for obtaining direct correlations between the hydrogen bond donor imino groups of uridine or guanine and the hydrogen bond acceptor N1 or N3 nitrogen atoms of adenine or cytosine, respectively. Hydrogen bonds with imino groups as donor and nitrogen atoms as acceptor also occur in a number of non-canonical base pairs. Examples include: (i) the „imino-hydrogen-bonded" or „G(anti) A(anti)" GA base pair observed in RNA molecules containing mismatches (4,5), in peptide–RNA complexes (6–8), in a tobramycin aptamer (9) and in a FMN aptamer complex (10); (ii) the reverse Hoogsteen AU base pair common to the family of RNA molecules containing the „E-loop motif" (11–13) or occurring in base triples (6,10); and (iii) GG base pairs observed in an ATP-aptamer structure (14,15). In the present paper we report the application of the HNN-COSY experiment to RNA molecules with non-canonical imino-hydrogen-bonded GA and reverse Hoogsteen AU base pairs.

## MATERIALS AND METHODS

### RNA synthesis and sample preparation

$^{15}N$-labeled nucleotide triphosphates were prepared, as described previously (16,17), from *Escherichia coli* grown on M9 minimal medium supplied with $^{15}N$ $NH_4Cl$ as the sole nitrogen source. $^{15}N$-labeled RNA molecules (hpGA, 5SDE and 5SE, see Fig. 1) were prepared by *in vitro* transcription

---

*To whom correspondence should be addressed. Tel: +49 3641 656217; Fax: +49 3641 656225; Email: mago@imb-jena.de

with T7 RNA polymerase (18,19) from either synthetic (MWG Biotech) double-stranded DNA (hpGA) or linearized plasmid DNA (5SDE, 5SE) templates containing the appropriate sequences. These molecules were purified on a DEAE Sepharose FF column (Amersham Pharmacia Biotech) developed with a sodium acetate step gradient and subsequently by HPLC on a preparative C18 column (Vydac 218TP510), equilibrated with 50 mM $KH_2PO_4/K_2HPO_4$ and 2 mM tetrabutylammonium hydrogen sulfate at pH 5.9 in water employing an acetonitrile gradient. In the case of hpGA and 5SDE a small amount of N+1 product was not separated from the main product. The 5SE template was fused to a hammerhead ribozyme sequence. The resulting transcript underwent self-cleavage at the 3' end of 5SE (20) and no additional products (N+1, N–1) were observed in this case. Lyophylized products were desalted with a NAP-25 gel filtration column (Amersham Pharmacia Biotech) and precipitated twice with 5 vol of 2% (w/v) lithium perchlorate in acetone. hpGA was denatured at 95°C at a concentration of 0.03 mM in 10-fold diluted NMR buffer (100 mM NaCl, 10 mM $NaH_2PO_4/Na_2HPO_4$, 2.5 mM EDTA, pH 6.9) and slowly cooled to room temperature over a period of 3 h. 5SDE and 5SE were folded into a monomeric hairpin form by denaturing at 95°C at a concentration of 0.25 mM and subsequent 5-fold dilution into ice cold water and finally exchanged into NMR buffer (5 mM $KH_2PO_4/K_2HPO_4$, 60 mM KCl and 8 mM $CaCl_2$, pH 5.75 for 5SDE or 20 mM $NaH_2PO_4/Na_2HPO_4$, 0.1 M KCl, 4 mM $MgCl_2$, 3 mM $NaN_3$, pH 7.2 for the 5SE–L25 complex) using Centricon-3 microconcentrators (Amicon, Inc.). Ribosomal protein L25 was prepared and the 5SE–L25 complex formed by titration as described previously (20). The final sample concentrations were ~1.7 mM for 5SDE and ~0.8 mM for hpGA and the 5SE–L25 complex.

## NMR spectroscopy

NMR experiments were performed on a Varian *UNITY INOVA* 600 MHz, a Varian *UNITY INOVA* 750 MHz or a Bruker DMX 600 MHz spectrometer. All spectra were processed and analyzed using Vnmr, Xeasy (21) and NMRpipe (22). NMR spectra were recorded in 95% $H_2O$/5% $D_2O$ at a temperature of 10°C (hpGA) or 25°C (5SDE and 5SE–L25 complex) using the WATERGATE (23) water suppression scheme including water flip-back pulses (24).

A $^1H$-$^1H$-NOESY spectrum was recorded at 750 MHz for hpGA with a data matrix consisting of 400 ($t_1$) × 960 ($t_2$) complex data points. Sweep widths of 9000 and 16 000 Hz in F1 and F2, respectively, and a NOE mixing time of 150 ms were used. A total of 128 scans per complex $t_1$ increment were collected. The $^1H$ carrier was positioned at 6.8 p.p.m. during $t_1$ and at the $H_2O$ resonance during $t_2$ and the $^{15}N$ carrier at 195 p.p.m. $^{15}N$ decoupling was employed during data acquisition. Data were zero filled to 4K × 4K complex data points and apodized using squared cosine functions in both dimensions before Fourier transformation.

3D $^1H$-$^1H$-$^{15}N$-NOESY-HSQC spectra were recorded at 750 MHz for 5SDE and the 5SE–L25 complex with 192 ($t_1$) × 44 ($t_2$) × 512 ($t_3$) complex data points, eight scans per increment, spectral widths of 11 300 Hz, 2190 Hz and 16 000 Hz in F1, F2 and F3, respectively, and a NOE mixing time of 80 ms. The $^1H$ carrier was positioned at 6.8 p.p.m. during $t_1$ and at the $H_2O$ resonance during acquisition. The $^{15}N$ carrier was positioned at 120 p.p.m. and $^{15}N$ decoupling was employed during acquisition. The data were zero filled to 1K × 128 × 1K
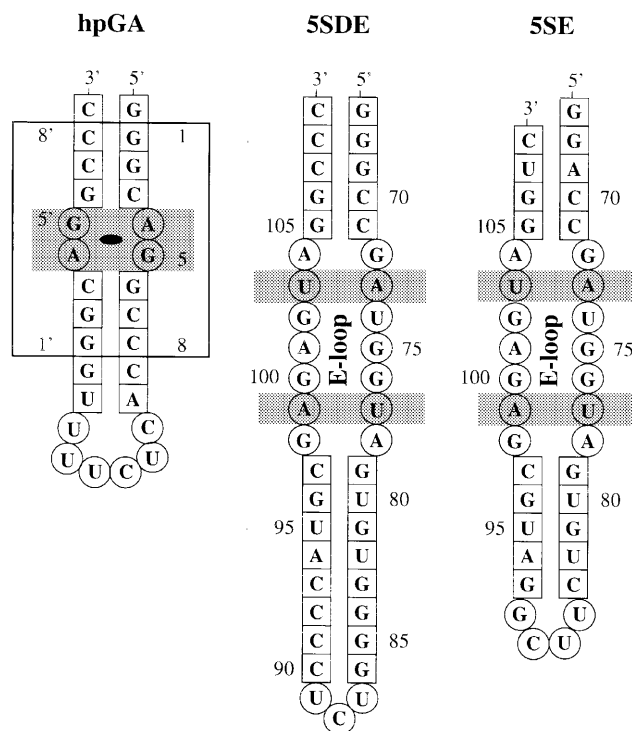


**Figure 1.** Sequences and secondary structures of the RNA molecules used in this study. Non-Watson–Crick base pairs with NH⋯N hydrogen bonds are shaded. hpGA, secondary structure of hpGA. The boxed region indicates the sequence studied by Wu *et al.* (4). The (pseudo) 2-fold symmetry axis of the molecule is indicated by a black oval. The numbering scheme is according to (4). 5SDE, secondary structure of 5SDE, which contains nucleotides 70–106 of *E.coli* 5S ribosomal RNA. 5SE, secondary structure of 5SE, which contains nucleotides 70–82 and 94–106 of *E.coli* 5S ribosomal RNA. The internal bulge region known as the E-loop is indicated for 5SDE and 5SE.

complex data points in F1, F2 and F3, respectively, and apodized using cosine functions in all dimensions before Fourier transformation.

The $^2J_{HN}$-$^1H$-$^{15}N$-HSQC experiments were recorded at 600 MHz either as a conventional WATERGATE (23) water flip-back (24) $^1H$-$^{15}N$-HSQC (hpGA) or according to Sklenar *et al.* (25) (5SDE, 5SE–L25 complex) with the INEPT transfer delays set to 10 ms. The data matrices consisted of 256 ($t_1$) × 800 ($t_2$) complex data points. A total of 64 scans per $t_1$ increment were collected. Spectral widths were 7000 Hz in the $^{15}N$ and 12 000 Hz in the $^1H$ dimension. The experiments were performed with the $^1H$ carrier positioned at the $H_2O$ resonance and the $^{15}N$ carrier at 195 p.p.m. The data were zero filled to 2K × 2K complex data points and apodized using cosine functions in both dimensions before Fourier transformation.

The quantitative $J_{NN}$ HNN-COSY experiments were performed as previously described (1). The data matrices consisted of 128 ($t_1$) × 800 ($t_2$) (5SE–L25 complex) or 350 ($t_1$) × 800 ($t_2$) complex data points (5SDE and hpGA). A total of 64 (5SDE, hpGA) or 256 (5SE–L25) scans per $t_1$ increment were collected. Spectral widths were 7000 Hz in the $^{15}N$ and 12 000 Hz in the $^1H$ dimension. The experiments were performed with the $^1H$ carrier positioned at the $H_2O$ resonance and the $^{15}N$ carrier at 153 p.p.m.
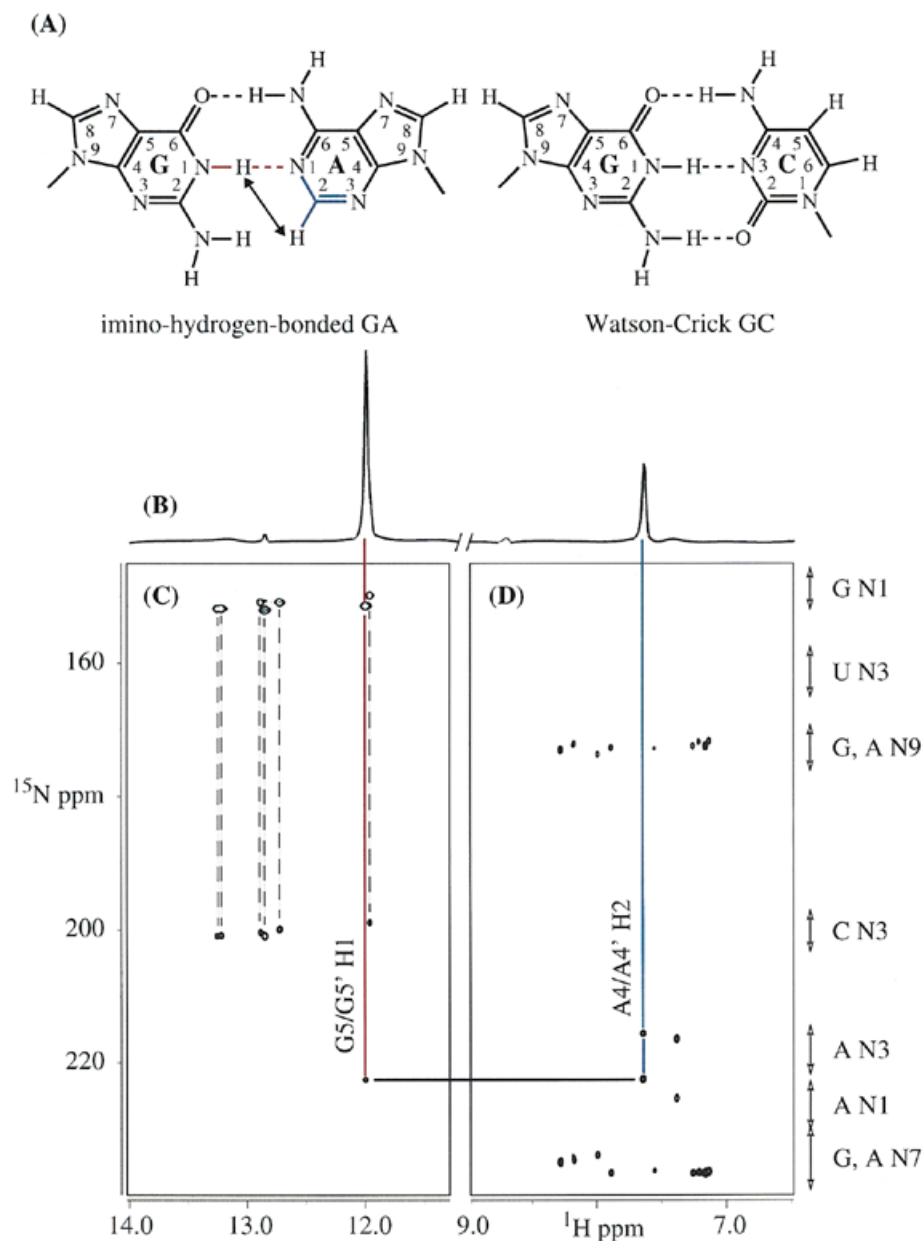
**Figure 2.** Assignment of a $^{2h}J_{NN}$ coupling in hpGA to a GA base pair with a G N1H1–A N1 hydrogen bond. (**A**) Geometry of an imino-hydrogen bonded GA base pair (left) in comparison with a Watson–Crick GC base pair (right). (**B**) One-dimensional cross section from a 2D $^1$H-$^1$H-NOESY spectrum taken at the chemical shift of the G5/G5′ H1 hydrogen showing the strong NOE cross peak to the A4/A4′ H2 hydrogen. (**C**) HNN-COSY spectrum of hpGA showing cross correlations between G H1 hydrogens and G N1 and C N3 nitrogens (dashed black lines) typical for Watson–Crick GC base pairs and between the G5/G5′ H1 hydrogen and the G5/G5′ N1 and A4/A4′ N1 nitrogens (red line). (**D**) $^2J_{HN}$-$^1$H-$^{15}$N-HSQC spectrum of hpGA showing the correlation of the A4/A4′ H2 hydrogen to the A4/A4′ N1 and N3 nitrogens (blue line). Typical chemical shift ranges of the relevant nitrogen atoms are indicated at the right side of the spectrum.

for the $^1$H-$^{15}$N-INEPT and at 194 p.p.m. during the NN-COSY step. A mixing time of 30 ms was used for the NN-COSY transfer. The data were zero filled to 512 × 2K complex data points and apodized using cosine functions in both dimensions before Fourier transformation. The quantification of the $^{2h}J_{NN}$-coupling constants was carried out as described previously without correcting for an underestimation of 10–20% due to the finite excitation bandwidth of the $^{15}$N radio frequency pulses (1).

## RESULTS

### A tandem GA mismatch in hpGA

The hpGA RNA molecule was constructed to allow the formation of a central, tandem GA mismatch (Fig. 1). A similar molecule (Fig. 1, boxed region) was studied previously (4) using $^1$H-$^1$H-NMR and complete relaxation matrix analysis. An imino hydrogen-bonded conformation of the two central GA base pairs (Fig. 2A) was inferred from strong NOEs between the G

H1 imino and the A H2 hydrogens. To improve the efficiency of the *in vitro* transcription procedure required for the incorporation of $^{15}$N-labeled nucleotides, we modified the sequence of the molecule studied by Wu *et al.* (4) by the introduction of extra base pairs and a loop sequence. The imino hydrogen spectrum of hpGA (data not shown) was very similar to that observed previously (4), indicating a similar structure for the helical regions of the two RNA molecules. Figure 2C shows the result of a HNN-COSY experiment for hpGA. Six correlations are observed for G H1 hydrogens with G N1 and C N3 nitrogens, indicating the presence of $^{2h}J_{NN}$ scalar couplings across the hydrogen bonds between the G N1 and C N3 nitrogens in Watson–Crick GC base pairs as described (1). Taking into account the (pseudo) 2-fold symmetry of the molecule and the patterns observed in the NOESY spectrum of this molecule (data not shown), these resonances could be assigned to the expected eight GC base pairs (Fig. 1, hpGA).

One G H1 hydrogen showed correlations both to a G N1 nitrogen and to a nitrogen at 222.60 p.p.m. This frequency is indicative of either adenine N1, N3 or purine N7 nitrogens (25). The adenine nitrogen nuclei N1 and N3 can be distinguished from the purine N7 nuclei in a $^{2}J_{HN}$-$^{1}$H-$^{15}$N-HSQC experiment (25). In this experiment, an adenine H2 hydrogen typically shows a correlation with two nitrogen resonances in the 215–225 p.p.m. range, which originate from the A N1 and A N3 nuclei (blue structure in Fig. 2A). In contrast, a purine H8 hydrogen is correlated with a N9 resonance at ~172 p.p.m. and a N7 resonance in the 225–240 p.p.m. range. The $^{1}$H-$^{15}$N-two-bond HSQC spectrum of hpGA (Fig. 2D) reveals that the resonance at 222.60 p.p.m. corresponds to an adenine N1. Furthermore, the G5/G5′ H1 imino hydrogen shows the expected strong NOE to the associated H2 hydrogen of this adenine (Fig. 2B), which is therefore assigned to A4/A4′. Thus, the observed $^{2h}J_{NN}$ coupling, with a calculated coupling constant of 5.0 Hz, is assigned to the symmetric G5N1–A4′N1/G5′N1–A4N1 nitrogens and directly demonstrates the presence of a hydrogen bond between the G N1H1 imino group as the donor and the A N1 nitrogen as the acceptor group. Given the (pseudo) symmetry of the molecule, this is strong evidence for a tandem GA mismatch with imino hydrogen bonded GA base pairs.

## Reverse Hoogsteen base pairs in 5SDE

The structure of the E-loop of 5S ribosomal RNA was recently studied by X-ray crystallography and NMR spectroscopy (26–28). Two central base pairs of this molecule (A73–U103 and U77–A99, Fig. 1) were identified as reverse Hoogsteen base pairs (Fig. 3A). The most conclusive evidence for hydrogen bonding between the U H3 imino hydrogen and the A N7 nitrogen was the short N3–N7 distance observed in the X-ray structure (26) and a strong NOE between the U H3 imino hydrogen and the A H8 hydrogen (27,28) (Fig. 3A). Further indirect evidence was provided by the strong protection from exchange with the solvent of the U H3 imino hydrogens as observed in the NMR studies (27,28).

In the HNN-COSY spectrum of 5SDE (Fig. 3B), seven correlations are observed for imino hydrogens with $^{15}$N resonances between 140 and 150 p.p.m. (G N1) and between 195 and 205 p.p.m. (C N3), as expected for the GC Watson–Crick base pairs in the helical stems of this molecule. Additionally, for the uridine imino H3 hydrogens of U82, U77 and U103, cross peaks are observed with the U N3 nitrogens as well as with
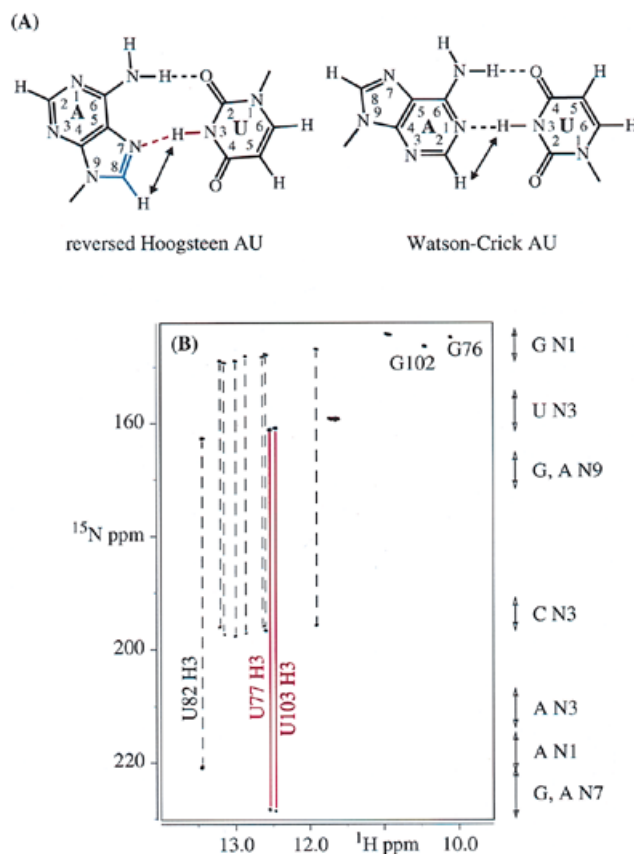


**Figure 3.** Observation of NH···N hydrogen bonds for the reverse Hoogsteen AU base pairs A73 N7–U103 N3H3 and U77 N3H3–A99 N7 in 5SDE. (**A**) Geometry of a reverse Hoogsteen AU base pair (left) in comparison with a Watson−Crick AU base pair (right). (**B**) HNN-COSY spectrum of 5SDE. Correlations of G N1 and C N3 with G H1 and of U82 N3 and A94 N1 with U82 H3 within Watson−Crick base pairs are indicated by dashed lines. Correlations of U77 H3 with U77 N3 and A99 N7 and of U103 H3 with U103 N3 and A73 N7 in the two reverse Hoogsteen AU base pairs are indicated by solid red lines.

nitrogens at chemical shifts above 220 p.p.m. corresponding to the chemical shift ranges for adenine N1 and N3 and purine N7 nitrogens. A $^{2}J_{HN}$-$^{1}$H-$^{15}$N-HSQC experiment (data not shown) identified the nitrogen resonance correlated with the U82 imino group as an adenine N1 as expected for the Watson–Crick A94–U82 base pair identified in previous structural studies (26–28). The nitrogen resonances correlated to the imino groups of U77 and U103 were identified as purine N7. Furthermore, the H8 hydrogens connected to these N7 nitrogens showed strong NOE cross peaks to the imino hydrogens (data not shown) as expected in a base pair with reverse Hoogsteen geometry (Fig. 3A). Thus, $^{2h}J_{NN}$ couplings have been observed between the A73 N7/U103 N3 and the A99 N7/U77 N3 nitrogens, thereby directly demonstrating the existence of the corresponding hydrogen bonds. $^{2h}J_{NN}$ coupling constants of 5.5 Hz were calculated for the A73/U103 and the U77/A99 base pairs. As expected, no NH···N correlations could be observed for the imino groups of the two „wobble" GU base pairs, since the acceptor nucleus is an oxygen. Furthermore, cross peaks were
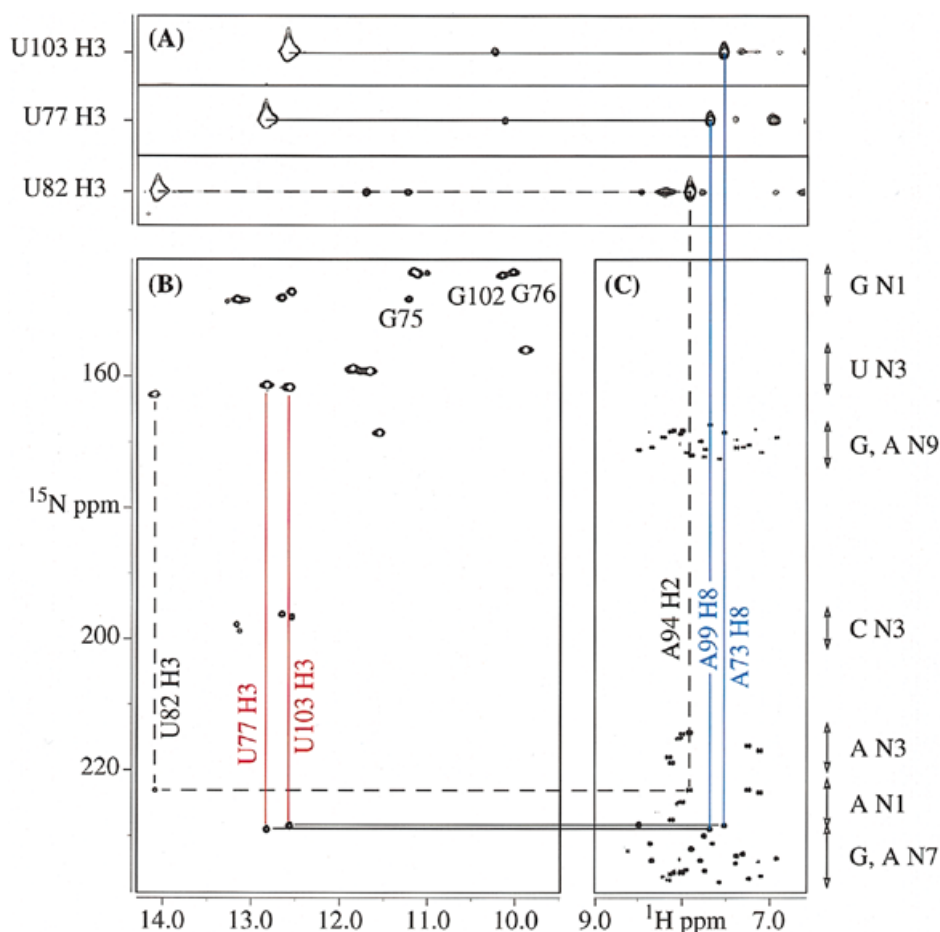
**Figure 4.** Observation of hydrogen bonds for the A73–U103 and U77–A99 reverse Hoogsteen base pairs and the U82–A94 Watson–Crick base pair in the 5SE–L25 complex. (**A**) $^1H$-$^1H$ slices from a three-dimensional $^1H$-$^1H$-$^{15}N$-NOESY-HSQC spectrum for U77, U103 and U82 showing the NOE cross peak between the U77/U103 imino H3 hydrogens and the A99/A73 H8 hydrogens of the reversed Hoogsteen AU base pairs (red line) and between the U82 imino H3 hydrogen and the A94 H2 hydrogen of the Watson−Crick AU base pair (dashed line), respectively. (**B**) HNN-COSY spectrum of the 5SE−L25 complex showing cross correlations of the U77/U103 H3 hydrogens with the U77/U103 N3 and A99/A73 N7 nitrogens (red lines) as well as between the U82 H3 hydrogens and the U82 N3 and A94 N1 nitrogens (dashed line). (**C**) $^2J_{HN}$-$^1H$-$^{15}N$-HSQC spectrum of the 5SE−L25 complex with the correlations of the A73/A99 H8 hydrogens to the A73/A99 N7 and N9 nitrogens (blue lines) and of the A94 H2 hydrogen to the A94 N1 and N3 nitrogens (dashed line), respectively.

absent in the HNN-COSY experiment for the other observable imino- and amino-groups in the E-loop region.

### Reverse Hoogsteen base pairs in the 5SE–L25 complex

No detailed structural information is currently available for the conformation of the E-loop when complexed with its cognate protein, ribosomal protein L25, but the possibility of conformational changes upon protein binding has been discussed (26,28,29). Therefore, we have used the HNN-COSY experiment to probe for the existence of the AU reverse Hoogsteen base pairs in the 5SE–L25 complex. Relative to the native DE domain of *E.coli* ribosomal 5S rRNA, 5SE (Fig. 1C) is shortened. However, with L25 it still forms a stable complex that is in slow exchange on the NMR timescale (20). The imino hydrogen spectrum of 5SE in complex with L25 has been assigned using several multi-dimensional NMR experiments (to be published). In the complex, as in the free RNA molecule, the imino hydrogens of U77 and U103 are protected against rapid exchange with the solvent. In the HNN-COSY experiment, the U77 and U103 H3 resonances show cross correlations to U N3 nitrogens and to nitrogens at 228.9 and 228.4 p.p.m., respectively (Fig. 4B, solid red lines). The $^2J_{HN}$-$^1H$-$^{15}N$-HSQC experiment identifies the resonances at 228.9 and 228.4 p.p.m. as N7 nitrogens and connects them to their attached H8 hydrogens (Fig. 4C, solid blue lines). The $^1H$-$^1H$-$^{15}N$-3D-NOESY-HSQC experiment shows that these H8 hydrogens exhibit intense NOE cross peaks to the uridine H3 imino hydrogens as expected for the reverse Hoogsteen base pairs (Fig. 4A). Therefore, in the 5SE–L25 complex, hydrogen bonds exist between the A73 N7/U103 N3H3 and the A99 N7/U77 N3H3 atoms. $^{2h}J_{NN}$ coupling constants of 5.5 Hz were calculated for the A73/U103 and the U77/A99 reverse Hoogsteen base pairs. The dashed lines in Figure 4 indicate the corresponding connectivities observed for the U82/A94 Watson–Crick base pair.

## DISCUSSION

In recent years the number of three-dimensional structures available for RNA molecules has increased considerably (30). From these studies it has become evident that non-canonical hydrogen bond interactions are often central to the formation and/or the maintenance of the functional, three-dimensional shape of these molecules. However, the existence of such hydrogen bonds generally had to be inferred indirectly from crystallographic or NMR structures rather than from direct spectroscopic correlation of the donor and acceptor groups of the hydrogen bonds in question. In the present paper, we have used RNA molecules containing imino-hydrogen bonded GA pairs or reverse Hoogsteen AU pairs to demonstrate that the recently established HNN-COSY experiment (1) can be used for the direct observation and identification of the hydrogen bond donor and acceptor groups involved in non-Watson–Crick NH···N hydrogen bonds. We have also shown that this approach is not only applicable to free RNA molecules of substantial size (43 nt in 5SDE), but also to sizeable RNA–protein complexes (37 nt, 94 amino acids in the 5SE–L25 complex).

To further assess the possibility of detecting unusual base pairs with the HNN-COSY experiment, and to further evaluate the extent to which binding of the ribosomal protein L25 may alter the conformation of the E-loop RNA, it is useful to note some of the characteristics of other NH hydrogens of the E-loop RNA in its complex with L25. A number of other imino hydrogens of the E-loop show slow exchange with solvent (Figs 3 and 4) and are therefore presumably stabilized against exchange by hydrogen bonds. In the previous structural studies, another unusual GA base pair (G75/A101) in the center of the E-loop was proposed to involve a water-mediated hydrogen bond between the imino group of G75 and the N1 nitrogen of A101 (26). The G75 H1 imino hydrogen of the GA pair is not detectable in the free form of the E-loop due to fast exchange with the solvent. However, it is detectable upon binding of the L25 protein (Fig. 4). In the proposed water-mediated hydrogen bond, the imino nitrogen and the acceptor nitrogen are separated by four chemical bonds and a relatively large distance of ~4.8 Å. Hence, the lack of a HNN cross correlation for the G75 N1H1 of the GA pair in the bound form of the E-loop (Fig. 4) does not contradict the preservation of such a water-mediated hydrogen bond.

Similarly, in the crystal structure of the E-loop RNA (26), the imino and amino groups of G102 and G76 are hydrogen bonded to the carbonyl O4 of U74 or the carbonyl O6 of G100, respectively, whereas the H3 and H1 imino hydrogens of U74 and G100 are not involved in a hydrogen bond. We observe slow exchange with the solvent for G76 and G102 in both the free and bound forms of the E-loop (Figs 3 and 4), but are unable to detect any NH···N hydrogen bonds in agreement with the previously proposed hydrogen bonding scheme. In previous structural studies of the free form of the E-loop (26–28), the two terminal base pairs of the loop, G72:A104 and A78:G98 were found to adopt a „sheared GA" geometry. In this base pairing scheme, hydrogen bonds which are of the NH···N type are formed between the G or A amino group and the A or G N7 nitrogen. In principle, these hydrogen bonds might be detectable in the HNN-COSY experiment. However, in 5SDE and the 5SE–L25 complex the two hydrogen atoms of the amino groups of these bases show a single resonance which is strongly broadened due to rotational exchange and/or exchange with the solvent. While the moderate exchange of these amino groups with solvent is suggestive of hydrogen bonding, any NH···N hydrogen bonds were not amenable to detection with the HNN-COSY experiment due to exchange broadening even at low temperatures. This type of behavior is not unusual for nucleotide amino groups and suggests that further stabilizing interactions, e.g. a second hydrogen bond from the amino group to a carbonyl function in a base triple, may be necessary to render NH···N hydrogen bonds involving donor amino groups detectable by the HNN-COSY experiment.

In short, for both the free and bound forms of the E-loop, a similar pattern of slow exchange and chemical shifts is observed for imino and amino hydrogens throughout the E-loop and direct evidence by $^{2h}J_{NN}$ couplings exists for hydrogen bond formation in the A73–U103 and U77–A99 reverse Hoogsteen base pairs. Although a full structural determination of the 5SE–L25 complex is still in progress, the present evidence appears to be consistent with the notion (26,28) that the unusual base pairs of the E-loop serve as a rigid docking module rather than undergoing an induced fit upon interaction with ribosomal protein L25.

From the present data it is evident that the HNN-COSY experiment is an efficient and sensitive tool not only for the direct detection of NH···N hydrogen bonds in canonical double-stranded regions of RNA (1), but also of this type of hydrogen bond in reverse Hoogsteen and G (anti) A (anti) base pairs. The values of the $^{2h}J_{NN}$ coupling constants in the GA mismatched pair and the reverse Hoogsteen AU base pairs are similar in size to those observed for Watson–Crick GC and AU pairs in A form RNA (1). This suggests that other non-canonical NH···N hydrogen bonds in RNA should also have values for the $^{2h}J_{NN}$ couplings in the range of 5–8 Hz. A compendium of 28 possible types of base pairs involving at least two hydrogen bonds (31) shows that 21 base pairs include hydrogen bonds of the NH···N type. Of these, eight involve imino groups and 13 involve amino groups as donors. Its is likely that $^{2h}J_{NN}$ correlations involving the amino function of bases will also be detectable if the amino group is sufficiently stabilized against rotation and/or solvent exchange. Therefore many of the NH···N hydrogen bonds should be detectable by the observation of trans-hydrogen bond scalar couplings. Such direct detection of hydrogen bonds in both canonical and non-canonical base pairs, which requires no prior knowledge of spatial relationships for the unambiguous identification of the participating donor and acceptor groups, will provide crucial information for accurate determination of three-dimensional RNA structures.

## ACKNOWLEDGEMENTS

## REFERENCES

1. Dingley,A.J. and Grzesiek,S. (1998) *J. Am. Chem. Soc.*, **120**, 1601–1602.
2. Pervushin,K., Ono,A., Fernandez,C., Szyperski,T., Kainosho,M. and Wüthrich,K. (1998) *Proc. Natl Acad. Sci. USA*, **95**, 14147–14151.
3. Cordier,F. and Grzesiek,S. (1999) *J. Am. Chem. Soc.*, **121**, 1601–1602.
4. Wu,M., SantaLucia,J.Jr and Turner,D.H. (1997) *Biochemistry*, **36**, 4449–4460.
5. Leonhard,G.A., McAuley-Hecht,K.E., Ebel,S., Lough,D.M., Brown,T. and Hunter,W.N. (1994) *Structure*, **2**, 483–494.
6. Ye,X., Gorin,A., Ellington,A.J. and Patel,D.J. (1996) *Nature Struct. Biol.*, **3**, 1026–1033.
7. Battiste,J.L., Mao,H., Rao,N.S., Tan,R., Muhandiram,D.R., Kay,L.E., Frankel,A.D. and Williamson,J.R. (1996) *Science*, **273**, 1547–1551.
8. Peterson,R.D. and Feigon,J. (1996) *J. Mol. Biol.*, **264**, 863–877.
9. Jiang,L. and Patel,D.J. (1998) *Nature Struct. Biol.*, **5**, 769–773.
10. Fan,P., Suri,A.K., Fiala,R., Live,D. and Patel,D.J. (1996) *J. Mol. Biol.*, **258**, 480–500.
11. Leontis,N.B. and Westhof,E. (1998) *J. Mol. Biol.*, **283**, 571–583.
12. Wimberly,B. (1994) *Nature Struct. Biol.*, **1**, 820–827.
13. Shen,L.X., Cai,Z. and Tinoco,I. (1995) *FASEB J.*, **11**, 1023–1033.
14. Jiang,F., Kumar,R.A., Jones,R.A. and Patel,D.J. (1996) *Nature*, **382**, 183–186.
15. Dieckmann,T., Suzuki,E., Nakamura,G.K. and Feigon,J. (1996) *RNA*, **7**, 628–640.
16. Batey,R.T., Inada,M., Kujawinski,E., Puglisi,J.D. and Williamson,J.R. (1992) *Nucleic Acids Res.*, **20**, 4515–4523.
17. Michnicka,M.J., Harper,J.W. and King,G.C. (1993) *Biochemistry*, **32**, 395–400.
18. Milligan,J.F., Groebe,D.R., Witherell,G.W. and Uhlenbeck,O.C. (1987) *Nucleic Acids Res.*, **15**, 8783–8798.
19. Grüne,M., Görlach,M., Soskic,V., Klussmann,S., Bald,R., Fürste,J.P., Erdmann,V.A. and Brown,L.R. (1996) *FEBS Lett.*, **385**, 114–118.
20. Stoldt,M., Wöhnert,J., Görlach,M. and Brown,L.R. (1998) *EMBO J.*, **17**, 6377–6384.
21. Bartels,C., Xia,T., Billeter,M., Güntert,P. and Wüthrich,K. (1995) *J. Biomol. NMR*, **6**, 1–10.
22. Delaglio,F., Grzesiek,S., Vuister,G.W., Zhu,G., Pfeifer,J. and Bax,A. (1995) *J. Biomol. NMR*, **6**, 277–293.
23. Piotto,M., Saudek,V. and Sklenar,V. (1992) *J. Biomol. NMR*, **2**, 661–665.
24. Grzesiek,S. and Bax,A. (1993) *J. Am. Chem. Soc.*, **115**, 12593–12594.
25. Sklenar,V., Peterson,R.D., Rejante,M.R. and Feigon,J. (1994) *J. Biomol. NMR*, **4**, 117–122.
26. Correll,C.C., Freeborn,B., Moore,P.B. and Steitz,T.A. (1997) *Cell*, **91**, 705–712.
27. Dallas,A., Rycyna,R. and Moore,P.B. (1995) *Biochem. Cell. Biol.*, **73**, 887–897.
28. Dallas,A. and Moore,P.B. (1997) *Structure*, **5**, 1639–1653.
29. Tang,R.S. and Draper,D.E. (1994) *Biochemistry*, **33**, 10089–10093.
30. Conn,G.L. and Draper,D.E. (1998) *Curr. Opin. Struct. Biol.*, **8**, 278–285.
31. Saenger,W. (1984) *Principles of Nucleic Acid Structure*. Springer-Verlag, New York, NY.